Mycol Progress (2014) 13:145–155
DOI 10.1007/s11557-013-0901-y

ORIGINAL ARTICLE

Two new species, *Pythium agreste* and *P. wuhanense*, based on morphological characteristics and DNA sequence data

Yan-Yan Long · Xin Sun · Ji-Guang Wei · Xiang Sun · Ji-Jing Wei · Hui Deng · Liang-Dong Guo

Received: 27 November 2012 / Revised: 13 March 2013 / Accepted: 23 March 2013 / Published online: 20 April 2013

Abstract In an investigation of *Pythium* species in China, two new species, *P. agreste* and *P. wuhanense*, were identified based on morphological characteristics and DNA sequence data. *Pythium agreste* has slightly inflated sporangia, oogonia encompassed by antheridia and antheridial stalks forming a very complicated knot, and plerotic oospores. It differs from the morphologically similar *P. volutum* which has inflated sporangia, bigger oogonia, and aplerotic oospores; from *P. kashmirense* which has contiguous inflated sporangia, catenulate oogonia and coiled or bent oogonial stalks; and from *P. pectinolyticum* which has catenulate oogonia and bigger oogonia and oospores. *Pythium wuhanense* can be differentiated from morphologically similar *P. emineosum* and *P. paroecandrum* by its possession of intercalary cylindrical to elongated sporangia and intercalary oogonia catenulate with sporangia and antheridia. Phylogenetic analyses showed that these two new species were clearly separated from morphologically similar *Pythium* species, based on the internal transcribed spacer (ITS) region and cytochrome C oxidase subunit I (COI) gene sequences using maximum parsimony and Bayesian methods. The two new species are described and illustrated in detail.

Keywords *Pythium agreste* · *Pythium wuhanense* · Morphology · COI · ITS

Xin Sun shared with the first author

Y.-Y. Long · J.-G. Wei (✉)
College of Agriculture, Guangxi University, Nanning 530005, People's Republic of China
e-mail: jiguangwei@gxu.edu.cn

X. Sun · X. Sun · L.-D. Guo (✉)
State Key Laboratory of Mycology, Institute of Microbiology, Chinese Academy of Sciences, Beijing 100101, People's Republic of China
e-mail: guold@sun.im.ac.cn

X. Sun
University of Chinese Academy of Sciences, Beijing 100049, People's Republic of China

J.-J. Wei
Changhe Agricultural Scientific Corporation, Dongguan 523070, People's Republic of China

H. Deng
Institute of Agricultural Resources and Regional Planning, Chinese Academy of Agricultural Sciences, Beijing 100081, People's Republic of China

Introduction

The genus *Pythium* Pringsheim, established in 1858, belongs to Pythiaceae, Peronosporales, Oomycetes, Oomycota and Straminipila (Hulvey et al. 2010). *Pythium* species are widely distributed throughout the world, and most species are saprobic in soil, water and the remains of dead plants and animals (van der Plaats-Niterink 1981). Some species are important pathogens of plants and animals and some can be beneficial as biological control agents protecting against pathogenic fungi (van der Plaats-Niterink 1981; Ali-Shtayeh and Saleh 1999).

Van der Plaats-Niterink (1981) revised the genus *Pythium* according to morphological characteristics, occurrence, and pathogenicity and accepted 87 species in this genus. More than 60 new *Pythium* species have been described since van der Plaats-Niterink's monograph (e.g., Senda et al. 2009; Uzuhashi et al. 2009; Bala et al. 2010; Long et al. 2010, 2012; Balghouthi et al. 2013). The taxonomy of *Pythium* is mainly based on the morphological characteristics such as the size and shape of oogonia, antheridia, and sporangia. However, some important morphological structures are highly variable, overlap considerably, and are absent in many species. These disadvantages contribute to the

historical lack of consensus on the most important morphological characteristics for species identification (Lévesque and De Cock 2004).

Molecular techniques have been employed in species identification and systematics of *Pythium*. The internal transcribed spacer (ITS) region of rDNA has been successfully used in the identification of *Pythium* species (e.g., Paul et al. 1998; Nechwatal and Oßwald 2003; Allain-Boulé et al. 2004; De Cock et al. 2008; Karaca et al. 2009), whereas there are identical ITS sequences in some morphologically distinct species (Lévesque and De Cock 2004; Long et al. 2010) and intra-specific heterogeneity of ITS sequences in other species (Kageyama et al. 2007; Belbahri et al. 2008; Mcleod et al. 2009; Senda et al. 2009). Bala et al. (2010) first combined the ITS region and cytochrome C oxidase subunit I (COI) gene to identify new *Pythium* species. Robideau et al. (2011) proposed that COI could be used as a primary DNA barcode and ITS as a supplementary barcode for Oomycetes. Therefore, *Pythium* species can be identified by a combination of morphological characteristics and ITS and COI sequence data (e.g., Nechwatal et al. 2005; Moralejo et al. 2008; Uzuhashi et al. 2009; Spies et al. 2011a, b; Long et al. 2012).

As part of an ongoing study of *Pythium* species diversity in China, two new species, *P. agreste* and *P. wuhanense*, were isolated and identified based on the morphological characteristics and ITS and COI sequence data in this study.

Materials and methods

Sample collection and isolation

Soil samples were collected from a sesame field in Liuyang (Hunan Province) and a paddy field in Wuhan (Hubei Province) in China in 2011. The samples were taken to the laboratory for isolation within 7 days. Oomycetes were isolated from the samples by putting soil particles on petri dishes with corn meal agar (CMA; see van der Plaats-Niterink 1981) directly; or by putting 2-cm-long sterilized grass (*Poa pratensis* L.) leaves on the surface of the soil sample soaked with sterilized water, to bait *Pythium* for 2–3 days. The colonized grass leaves were then transferred to CMA, and incubated at 25 °C. When mycelial growth was observed, purification was carried out by cutting a small piece of medium with mycelia at the edge of a colony, and transferring this onto new medium plates.

Morphology and growth rate

The purified isolates were grown on CMA for morphological observation and transferred to sterilized distilled water for sporulation. Approximately 30 measurements were taken for each morphological characteristic, such as sporangia, oogonia, and oospores.

The cardinal temperatures were examined on potato carrot agar (PCA; see van der Plaats-Niterink 1981) according to the method of Tojo et al. (2012) with modifications. The isolates were incubated at 0–45 °C with intervals of 5 °C on PCA. When no growth was observed at a certain temperature, the interval between growth and no growth was reduced from 5 to 2 °C or to 1 °C to determine the minimum and maximum growth temperatures. The growth rate was evaluated by visual measurement of the colony along its longest perpendicular diameter incubated at 24 h on PCA with three replicates.

DNA extraction, PCR and sequencing

Isolates of *Pythium* species were cultured on potato dextrose agar (PDA; see Guo et al. 2000) at 25 °C for 3–5 days. Genomic DNA was extracted from fresh cultures following the protocol of Guo et al. (2000). The ITS region was amplified with universal primer pairs ITS5 and ITS4 (White et al. 1990). The COI gene was amplified with primer pairs FM52R (5′-TTAGAATGGAATTAGCACAAC-3′, reversed the complementation of FM52) and FM55 (5′-GGCATACC AGCTAAACCTAA-3′, Martin 2000). Amplification was performed in a 50-μL reaction volume which contained PCR buffer [20 mM KCl, 10 mM $(NH_4)_2SO_4$, 2 mM $MgCl_2$, 20 mM Tris–HCl, pH8.4], 200 μM of each deoxyribonucleotide triphosphate, 15 pmols of each primer, 100 ng template DNA, and 2.5 units of *Taq* DNA polymerase (Biocolor BioScience and Technology, Shanghai, China). The thermal cycling program was as follows: 3 min initial denaturation at 95 °C, followed by 35 cycles of 40 s denaturation at 94 °C, 50 s annealing at 54 °C, 60 s extension at 72 °C, and a final 10 min extension at 72 °C. A negative control using sterilized distilled water instead of template DNA was included in the amplification process. The PCR products were examined by electrophoresis at 75 V for 2 h in 0.8 % (W/V) agarose gel in 1×TAE buffer (0.4 M Tris, 50 mM NaOAc, 10 mM EDTA, pH 7.8) and visualized under ultraviolet light after staining with ethidium bromide (0.5 μg ml^{-1}). The PCR products were purified using PCR Cleanup Filter Plates (MultiScreen® PCRμ96; Millipore, USA) according to the manufacturer's protocol. Purified PCR products were directly sequenced with primer pairs as mentioned above in an ABI 3730-XL DNA sequencer (Applied Biosystems, USA).

Phylogenetic analysis

The sequences of ITS and COI obtained in this study and reference taxa downloaded from GenBank were aligned with MAFFT using the G-INS-i option (Katoh et al. 2005). All sites were treated as unordered and unweighted, and gaps were treated as missing data in the phylogenetic

analyses. Maximum parsimony analyses of the alignment dataset of ITS and COI sequences were conducted with the heuristic search algorithm with tree-bisection-reconnection branch swapping in PAUP 4.0b10 (Swofford 2002). For each search, 1,000 replicates of random stepwise sequence addition were performed and all trees were saved per replicate. The strength of the internal branches of the trees was tested with bootstrap analysis using 1,000 replications with the same search setting.

Bayesian analyses of the same aligned ITS and COI dataset were conducted with MrBayes 3.1.2 (Huelsenbeck and Ronquist 2001), following the protocol of Sun and Guo (2010). The best-fit evolutionary model was determined for each dataset by comparing different evolutionary models via MrModeltest 2.3 (Nylander 2008). Four simultaneous chains of Markov Chain Monte Carlo were run starting from random trees and sampling every 100 generations. The analyses were halted at 1,000,000 generations for ITS and COI sequences, when the calculation reached stationarity. At the end of the analysis, 10,000 trees were generated, respectively, and 25 % of them were excluded as the "burn in" when calculating the posterior probabilities. Bayesian posterior probabilities were obtained from the 50 % majority rule consensus trees that remained. If more than 95 % of the sampled trees contained a given clade, it was considered to be significantly supported by our data.

Results

Taxonomy

Pythium agreste Y.Y. Long, *J.G. Wei* & *L.D. Guo* sp. nov. (Fig. 1)

MycoBank. MB 801477.

Etymology This oomycete is named as *P. agreste* because its holotype strain was isolated from soil of agricultural system.

Holotype China, Hunan Province, Liuyang, 28°20′N, 113°23′E, 100 m asl., from the soil of a sesame field, Y.Y.

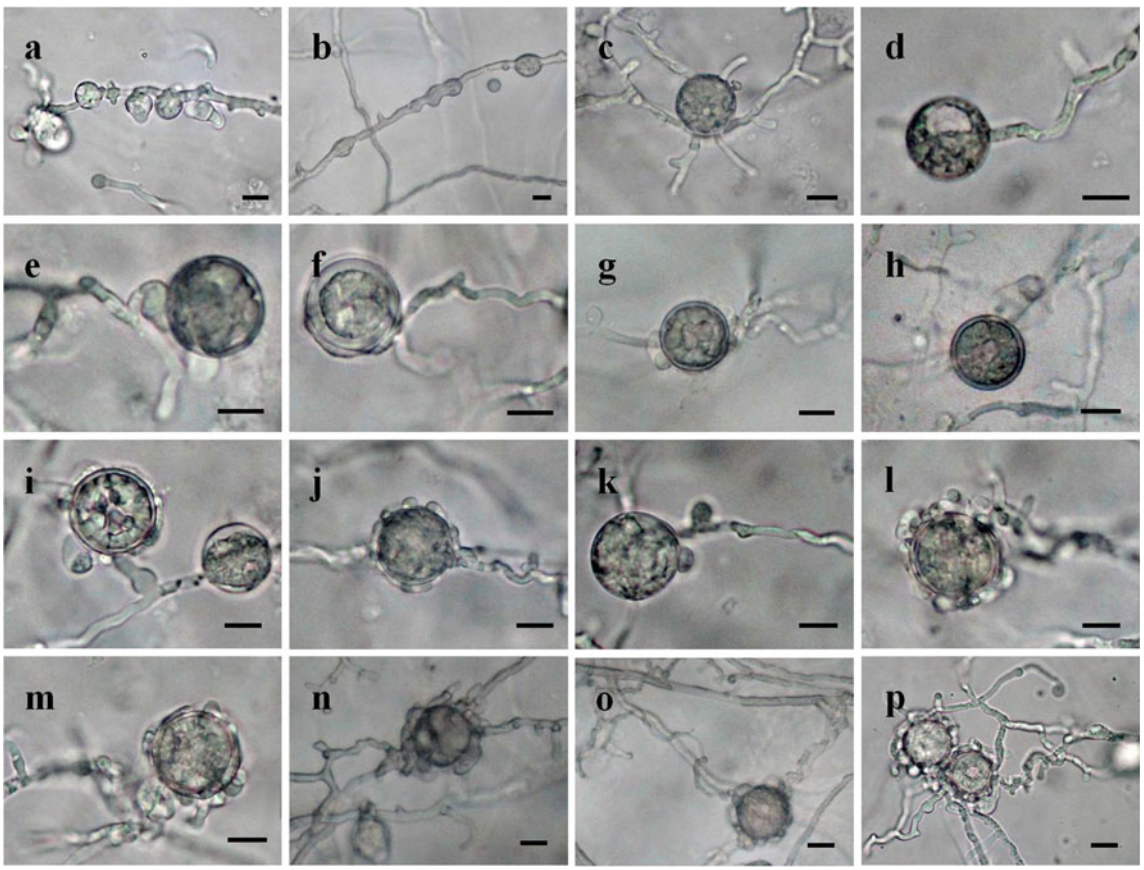

Fig. 1 Asexual and sexual reproductive bodies of *Pythium agreste*. **a** Sporangia with small lobes and toruloid outgrowths; **b** slightly inflated sporangium; **c** hyphal body with germ tubes; **d** subterminal hyphal body; **e** two sessile antheridia applied to oogonium; **f** nearly plerotic oospore with thick wall; **g** diclinous antheridium making lateral contact with oogonium; **h** diclinous antheridium making broad apical contact with oogonium; **i** plerotic oospore and antheridium with short stalk; **j** oogonium surrounded by antheridial stalks and antheridia; **k** terminal oogonium; **l**–**n** branched antheridial stalks bearing 1–2 antheridial cells and vegetative prolongations entangling the oogonium; **o**, **p** diclinous antheridia with stalks entwining oogonial stalk. *Scale bar* 10 μm

Long, 3. 8. 2011. Holotype (HMAS243737) deposited in the Herbarium Mycologicum Institute Microbiologici Academiae Sinicae (HMAS). Living culture (CGMCC3.15150) deposited in China General Microbiological Culture Collection Center (CGMCC).

This oomycete grew well on CMA, PCA, and PDA. Mycelia hyaline, branched, up to 4.5 μm wide. Colonies on PCA submerged, with a mixed rosette and chrysanthemum pattern. Average growth rate 10 mm day^{-1} at 25 °C. Cardinal temperature, minimum 4 °C, optimum 28 °C, maximum 42 °C. Appressoria not observed. Zoospores formed in sterile water at 20–28 °C. Sporangia filamentous, slightly inflated, sometimes with small lobes and toruloid outgrowths. Hyphal bodies globose or subglobose, mostly intercalary, sometimes terminal or subterminal, 10–22.5 μm (15.7±3.1 μm, n=32) diam. Female gametangia (oogonia) globose, smooth-walled, terminal or intercalary, filled with dense, coarsely granulated protoplasm, 16.3–27.5 μm (19.1±2.7 μm, n=33) diam. Male gametangia (antheridia) 1–3(4) per oogonium, mostly diclinous, at times monoclinous, often crowding around oogonia with antheridial stalks forming a very complicated knot. Antheridial stalks often branched, arising at various distances from oogonia, sometimes entwining the oogonial stalks. Antheridial cells club-shaped or fist-shaped, making broad apical or lateral contact with oogonia. Oospores 1 per oogonium, plerotic or nearly plerotic, globose, colorless, 16.3–25 μm (18.7±2.1 μm, n=32) diam.

Pythium wuhanense Y.Y. Long, J.G. Wei &L.D. Guo sp. nov. (Fig. 2)

MycoBank. MB 801479

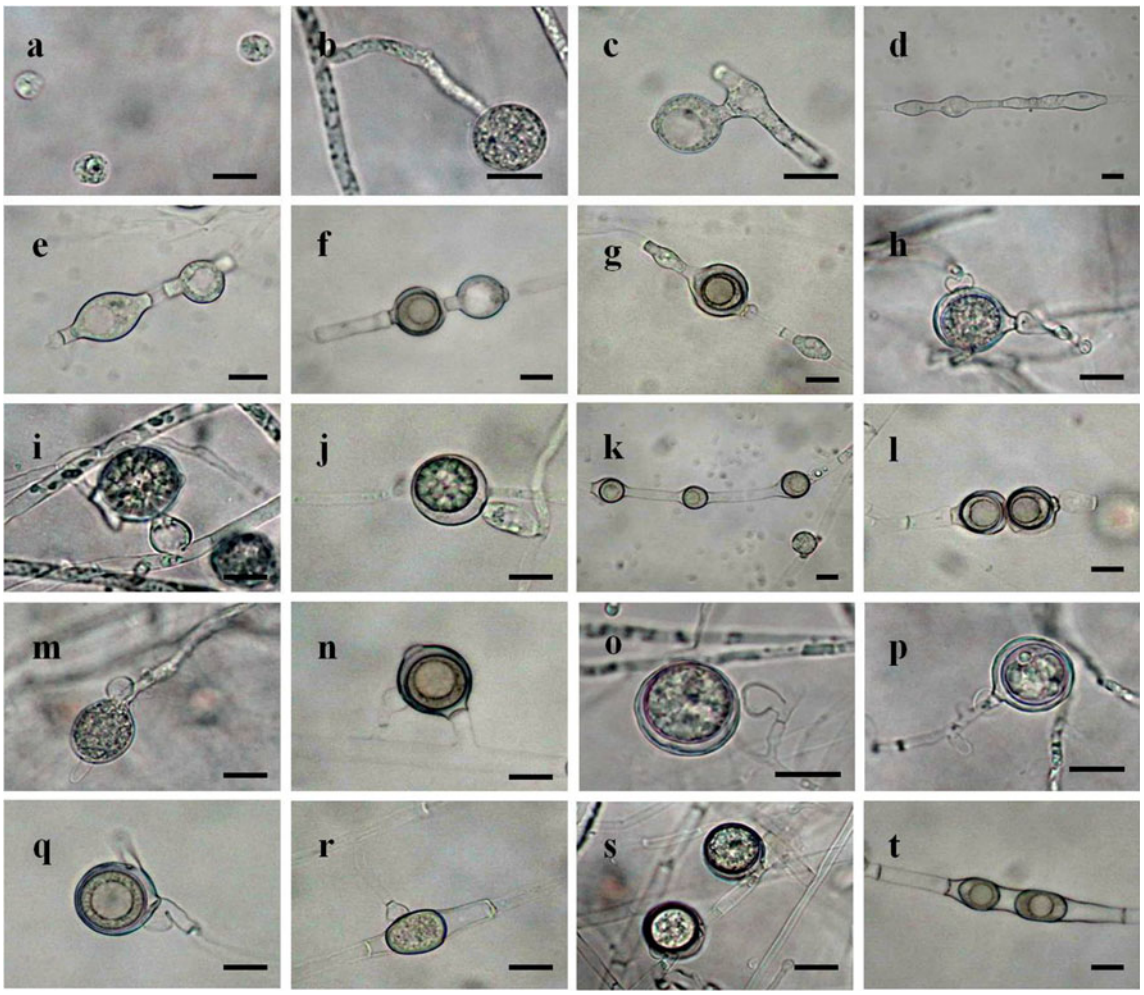

Fig. 2 Asexual and sexual reproductive bodies of *Pythium wuhanense*. **a** Released zoospores; **b** terminal globose sporangium; **c** globose sporangium catenulate with cylindrical sporangium; **d** elongated sporangium; **e** catenulate globose sporangia; **f**–**g** globose oogonia catenulate with sporangia and antheridia; **h** diclinous stalked antheridium and hypogynous antheridium; **i** lateral oogonium and intercalary antheridium; **j** intercalary antheridium making narrow apical contact with oogonium; **k**, **l** catenulate oogonia; **m** subterminal oogonium; **n** intercalary oogonium and diclinous antheridium with short stalk; **o** fist-shaped antheridium making broad apical contact with oogonium; **p** terminal oogonium with monoclinous sessile antheridium; **q** lobate antheridium; **r** elongate oogonium and oval oospore; **s** intercalary oogonium catenulate with lateral oogonium; **t** two ellipsoidal oospores in an elongate oogonium. *Scale bar* 10 μm

Etymology The oomycete is named as *P. wuhanense* because its holotype strain was isolated from the soil sample collected in Wuhan.

Holotype China, Hubei Province, Wuhan, 30°34′N, 113°53 E, 21.5–26 m asl., from the soil of a paddy field, Y.Y. Long, 28. 4. 2011, Holotype (HMAS243736) deposited in the Herbarium Mycologicum Institute Microbiologici Academiae Sinicae. Living culture (CGMCC3.15149) deposited in China General Microbiological Culture Collection Center.

This oomycete grew well on CMA, PCA and PDA. Mycelia hyaline, branched, up to 7.5 μm diam. Colonies on PCA have a vague radiate pattern with some arachnoid aerial mycelia. Average growth rate 50 mm day^{-1} at 25 °C. Cardinal temperatures, minimum 4 °C, optimum 28–30 °C, maximum 35 °C. Appressoria vermiform, rarely observed. Zoospores formed in sterile water at 25 °C. Sporangia mostly globose, sometimes cylindrical to elongated and mainly intercalary, often catenulate with oogonia, occasionally terminal or lateral; globose sporangia 11.3–25.5 μm (18.1±3.3 μm, n=31) in diameter, elongated sporangia up to 130 μm long. Female gametangia (oogonia) globose, but often including part of the oogonial stalk, sometimes cylindrical to elongated, smooth-walled, occasionally provided with a hyaline papilla; mostly intercalary, often catenulate with sporangia and antheridia, sometimes terminal or lateral, at times subterminal, filled with dense, coarsely granulated protoplasm; globose oogonia 10–20 μm (17.7±2.7 μm, n= 30) in diameter, elongated oogonia up to 64 μm long. Male gametangia (antheridia) 1–2 per oogonium, monoclinous, sessile, hypogynous, intercalary or diclinous. Antheridial stalks unbranched, arising at various distances from oogonia. Antheridial cells club-shaped, fist-shaped, sometimes lobate, making broad or narrow apical contact with oogonia. Oospores 1(2) per oogonium, most aplerotic, occasionally nearly plerotic, globose, occasionally oval or ellipsoidal, colorless; globose oospores 7.5–17.5 μm (14.5± 2.4 μm, n=30) in diameter, elongated oospores up to 42.5 μm long.

Phylogenetic analysis

In order to determine the phylogenetic positions of the new species, *P. agreste* and *P. wuhanense*, all available ITS and COI sequences of *Pythium* species in GenBank were downloaded. The maximum parsimony (MP) analyses indicated that *P. agreste* and *P. wuhanense* belonged to clade A and clade F, respectively (data not shown). For *P. agreste*, the COI gene sequences of *P. agreste*, 15 isolates from clade A, and two taxa from clade B1, used as the outgroup, were included in the phylogenetic analysis. In the alignment of the 18 COI sequences, the data matrix comprised 547 characters, of which 90 (16.5 %) were parsimony informative. The maximum parsimony analysis of the alignment dataset was subjected to a heuristic search for the most parsimonious trees and a strict consensus tree was obtained from seven equally most parsimonious trees (CI=0.7086, RI=0.8610, RC=0.6101, HI=0.2914). The same alignment dataset was also performed using the MrBayes program, applied with GTR+I model selected by MrModeltest as the best-fit model. The prior probability density is a flat Dirichlet (all values are 1.0) for both Revmatpr and Statefreqpr as default settings. A Bayesian tree with posterior probability (BPP) and parsimony bootstrap values at branches is shown in Fig. 3. In the phylogenetic tree, *P. agreste* formed a clade with *P. porphyrae* Takah & Sasaki, *P. chondricola* De Cock and *P. adhaerens* Sparrow with 1.00 support of BPP and 63 % support of MP.

Meanwhile, the ITS sequences of *P. agreste*, 15 isolates from clade A and two taxa from clade B1, used as the outgroup, were included in the phylogenetic analysis. In the alignment of the 18 ITS sequences, the data matrix comprised 839 characters, of which 152 (18.1 %) were parsimony informative. The maximum parsimony analysis of the alignment dataset was subjected to a heuristic search for the most parsimonious trees and one parsimonious tree was created (CI=0.8258, RI=0.9327, RC=0.7702, HI= 0.9327). The same alignment dataset was also performed using MrBayes program, applied with GTR+I+G model selected by MrModeltest as the best-fit model. The prior

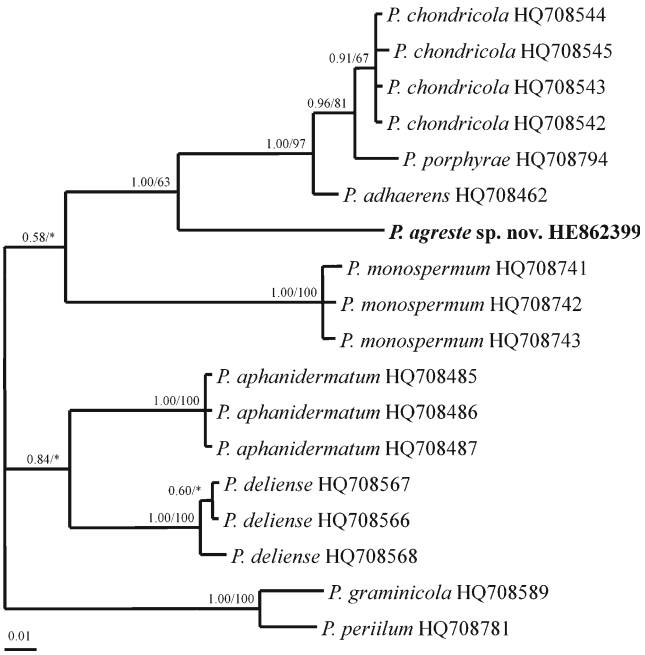

Fig. 3 Bayesian tree based on COI gene sequences showing the relationship of *P. agreste* with *Pythium* species in clade A (see Lévesque and de Cock 2004). *Pythium graminicola* and *P. periilum* from clade B1 were designated as outgroups. The *numbers at each branch point* represented Bayesian posterior probabilities (*left*) and percentage bootstrap support calculated from 1,000 replicates (*right*). *indicates lack of support or support less than 50 % for a particular clade. *Bar* 0.1 expected changes per site

probability density is a flat Dirichlet (all values are 1.00) for both Revmatpr and Statefreqpr as default settings. A Bayesian tree with posterior probability and parsimony bootstrap values at branches is shown in Fig. 4. In the phylogenetic tree, *P. agreste* also formed a clade with *P. porphyrae*, *P. chondricola*, and *P. adhaerens* with high bootstrap values (1.00 support of BPP and 94 % support of MP).

For *P. wuhanense*, the COI gene sequences of *P. wuhanense*, 20 isolates from clade F and two taxa from clade E, used as the outgroup, were included in the phylogenetic analysis. In the alignment of the 23 COI sequences, the data matrix comprised 545 characters, of which 62 (11.4 %) were parsimony informative. The maximum parsimony analysis of the alignment dataset was subjected to a heuristic search for the most parsimonious trees and a strict consensus tree was obtained from 106 equally most parsimonious trees (CI=0.5954, RI=0.6698, RC=0.3988, HI=0.4046). The same alignment dataset was also performed using the MrBayes program, applied with GTR+I+G model selected by MrModeltest as the best-fit model. The prior probability density is a flat Dirichlet (all values are 1.0) for both Revmatpr and Statefreqpr as default settings. A Bayesian tree with posterior probability and parsimony bootstrap values at branches is shown in Fig. 5. In the phylogenetic tree, *P. wuhanense* formed a clade with *P.* sp. P19448 and *P.* sp. P19510 with 0.96 support of BPP and 70 % support of MP.

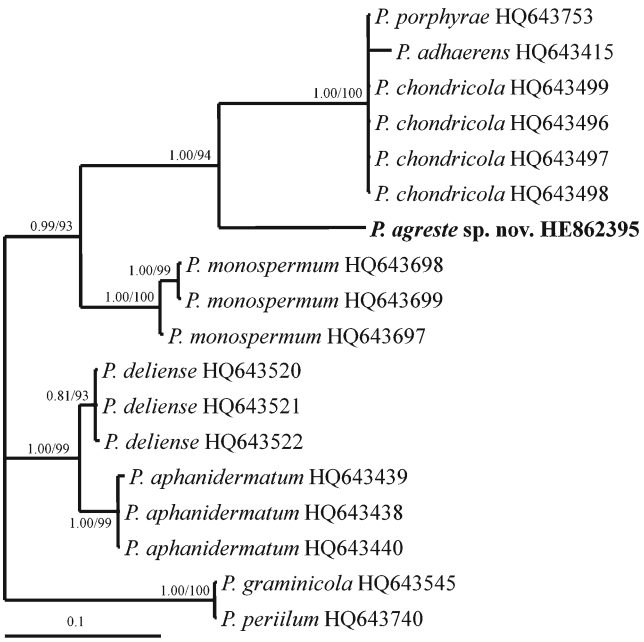

Fig. 4 Bayesian tree based on ITS (ITS1, 5.8S, ITS2) region sequences showing the relationship of *P. agreste* with *Pythium* species in clade A (see Lévesque and de Cock 2004). *Pythium graminicola* and *P. periilum* from clade B1 were designated as outgroups. The *numbers at each branch point* represented Bayesian posterior probabilities (*left*) and percentage bootstrap support calculated from 1,000 replicates (*right*). *indicates lack of support or support less than 50 % for a particular clade. *Bar* 0.1 expected changes per site

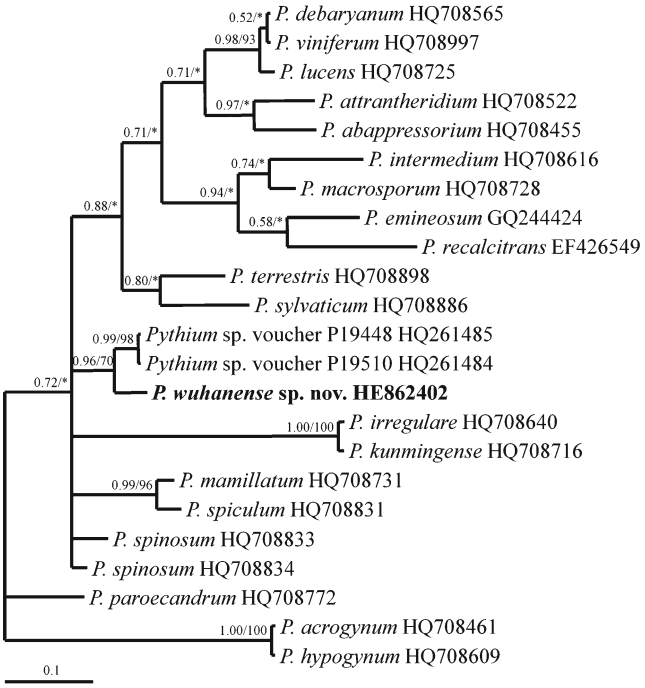

Fig. 5 Bayesian tree based on COI gene sequences showing the relationship of *P. wuhanense* with *Pythium* species in clade F (see Lévesque and de Cock 2004). *Pythium acrogymum* and *P. hypogynum* from clade E were designated as outgroups. The *numbers at each branch point* represented Bayesian posterior probabilities (left) and percentage bootstrap support calculated from 1,000 replicates (*right*). *indicates lack of support or support less than 50 % for a particular clade. *Bar* 0.1 expected changes per site

The ITS sequences of *P. wuhanense*, 20 isolates from clade F and two taxa from clade E, used as the outgroup, were included in the phylogenetic analysis. In the alignment of the 23 ITS sequences, the data matrix comprised 1005 characters, of which 342 (34.0 %) were parsimony informative. The maximum parsimony analysis of the alignment dataset was subjected to a heuristic search for the most parsimonious trees and one parsimonious tree was created (CI=0.7433, RI=0.7979, RC=0.5931, HI=0.2567). The same alignment dataset was also performed using the MrBayes program, applied with GTR+G model selected by MrModeltest as the best-fit model. The prior probability density is a flat Dirichlet (all values are 1.0) for both Revmatpr and Statefreqpr as default settings. A Bayesian tree with posterior probability and parsimony bootstrap values at branches is shown in Fig. 6. In the phylogenetic tree, *P. wuhanense* formed a clade with *P. spinosum* Sawada and *P. kunmingense* Yu with 100 % support of BPP and 71 % support of MP.

Discussion

The new species, *P. agreste*, is characterized by filamentous or slightly inflated sporangia, smooth oogonia encompassed

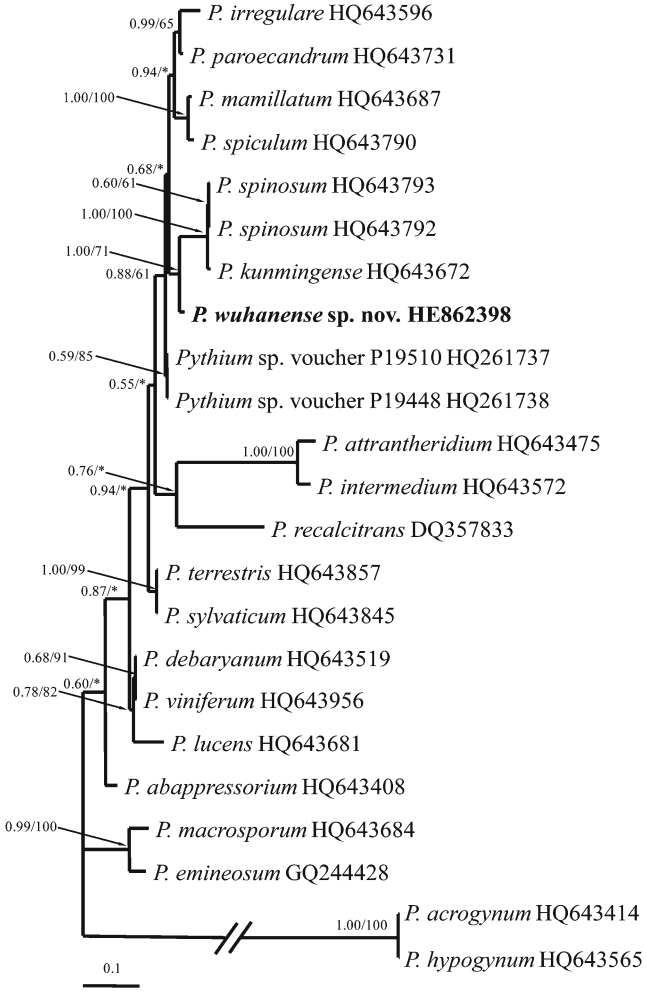

Fig. 6 Bayesian tree based on ITS (ITS1, 5.8S, ITS2) region sequences showing the relationship of *P. wuhanense* with *Pythium* species in clade F (see Lévesque and de Cock 2004). *Pythium acrogymum* and *P. hypogynum* from clade E were designated as outgroups. The *numbers at each branch point* represented Bayesian posterior probabilities (*left*) and percentage bootstrap support calculated from 1,000 replicates (*right*). *indicates lack of support or support less than 50 % for a particular clade. *Bar* 0.1 expected changes per site

by antheridial stalks forming a very complicated knot, long antheridial stalks entwining the oogonial stalks, and plerotic or nearly plerotic oospores. Among the *Pythium* species with filamentous sporangia, *P. agreste* is morphologically similar to *P. kashmirense* Paul and *P. volutum* Vanterpool & Truscott due to the presence of antheridial stalks entwining the oogonial stalks. However, *P. agreste* differs from *P. kashmirense* which has contiguous inflated sporangia, catenulate and smaller oogonia (average 19.1 vs. 16.4 μm in diameter), coiled or bent oogonial stalks and more antheridia (1–3 vs. 1–6 per oogonium), and from *P. volutum* which has inflated sporangia, bigger oogonia (average 19.1 vs. 30 μm), bigger oospores (average 18.7 vs. 27.5 μm in diameter) and more antheridia (1–3 vs. 3–6 per oogonium) (Table 1). In addition, *P. agreste* is also morphologically similar with *P. pectinolyticum* Paul through the presence of antheridia crowding around oogonia, but *P. agreste* can be differentiated from *P. pectinolyticum* which has catenulate and bigger oogonia (average 19.1 vs. 30.3 μm in diameter) and bigger oospores (average 18.7 vs. 27.3 μm in diameter) (Table 1). Furthermore, the results of the phylogenetic analyses of ITS and COI sequences indicated that *P. agreste* was clearly separated from these three morphologically similar species (Figs. 3. 4).

In addition, the phylogenetic analysis results indicated that *P. agreste* had closer relationships with *P. adhaerens*, *P. chondricola*, and *P. porphyrae* compared to the other species (Figs. 3, 4), but *P. agreste* had low DNA sequence similarities with *P. adhaerens* (91.5 % ITS identity with HQ643415 and 93.3 % COI identity with HQ708462), *P. chondricola* (92.4 % ITS identity with HQ643498 and 92.6 % COI identity with HQ708544), and *P. porphyrae* (92.2 % ITS identity with HQ643753 and 92.1 % COI identity with HQ708794). Furthermore, in morphology, *P. agreste*, with slightly inflated filamentous sporangia, differs from *P. adhaerens*, *P. chondricola*, and *P. porphyrae*, all of which lack inflated filamentous sporangia. In addition, *P. agreste*, with plerotic or nearly plerotic oospores, can be differentiated from *P. adhaerens* with its aplerotic oospores. Also, *P. agreste*, with mostly terminal oogonia encompassed by antheridia and antheridial stalks, differs from *P. chondricola* and *P. porphyrae* which have mostly intercalary oogonia (Table 1).

The new species, *P. wuhanense*, is characterized by intercalary cylindrical to elongated sporangia, intercalary cylindrical to elongated oogonia catenulate with sporangia and antheridia, and various types of antheridial contacts with oogonia. Among the *Pythium* species with globose sporangia and smooth oogonia, *P. wuhanense* is morphologically similar to *P. emineosum* Bala, De Cock & Lévesque by the presence of elongated oogonia, two oospores, and various types of antheridial contacts with the oogonia; and with *P. paroecandrum* Drechsler by possessing intercalary sporangia, catenulate oogonia, and various types of antheridial contacts with the oogonia (Table 2). However, *P. wuhanense*, has intercalary oogonia catenulate with sporangia and antheridia and a faster growth rate, and thus can be differentiated from *P. emineosum* and *P. paroecandrum*. In addition, *P. wuhanense*, with aplerotic oospores, differs from *P. emineosum* with plerotic oospores, and from *P. paroecandrum* which has bigger globose oogonia (average 19 vs. 17.7 μm in diameter) and oospores (average 17 vs. 14.5 μm in diameter). Furthermore, the results of the phylogenetic analyses of ITS and COI sequences indicated that *P. wuhanense* was clearly separated from these two morphologically similar species.

In addition, the phylogenetic analysis of COI sequences indicated that *P. wuhanense* had closer relationships with *Pythium* sp. P19448 and *Pythium* sp. P19510 compared with the other species (Fig. 5), but we cannot compare the

Table 1 A comparison of *Pythium agreste* with related species

Character	*P. agreste*	*P. adhaerens*	*P. chondricola*	*P. kashmirense*	*P. pectinolyticum*	*P. porphyrae*	*P. volutum*
Growth rate on PCA	10 mm day^{-1} at 25 °C	5 mm day^{-1} at 25 °C	3–4 mm after a lag period of some days at 25 °C	15 mm day^{-1} at 25 °C	7 mm day^{-1} at 25 °C	no growth	10 mm day^{-1} at 25 °C
Sporangia	Filamentous, slightly inflated or with small lobes and toruloid outgrowths	Filamentous non-inflated	Filamentous non-inflated	Filamentous inflated, contiguous and linked to each other by thin filaments	Filamentous, slightly thicker than vegetative hyphae	Filamentous non-inflated	Filamentous inflated, with small lobes and toruloid outgrowths
Oogonia	Globose, smooth, 16.3–27.5 µm (av. 19.1 µm) in diameter, terminal or intercalary	Globose, smooth, 11–25 µm (av. 17.5 µm) in diameter, terminal or intercalary	Globose to subglobose, smooth or with undulate wall, (14)16–24(34) µm (av. 25.3 µm) in diameter, mostly intercalary	Globose, smooth, 11–22 µm (av. 16.4 µm) in diameter, mostly intercalary or catenulate	Globose, smooth, 25–40 µm (av. 30.3 µm) in diameter, terminal, sub-terminal, intercalary or catenulate	Globose, smooth, 14.5–19.5 µm, intercalary	Globose or subglobose, smooth, on average 30 µm in diameter, terminal
Antheridia	1–3(4) mm per oogonium, mostly diclinous, often crowding around oogonia. Antheridial stalks often branched, sometimes entwining oogonia or oogonial stalks. Antheridial cells club-shaped or fist-shaped	1–4 per oogonium, diclinous, often encircling oogonia. Antheridial stalks rarely branched. Antheridial cells crook-necked	1–3(4) per oogonium, diclinous. Antheridial stalks sometimes branched. Antheridial cells sac-like to club-shaped	1–6 per oogonium, diclinous. Antheridial stalks coiling around oogonial stalks in loose loops or around oogonia with loose or tight loops. Antheridial cells club-shaped	Usually absent. When present, crowding around oogonia, difficult to determine their origin, type of contact and numbers	1–2(4) per oogonium, diclinous. Antheridial stalks unbranched. Antheridial cells globose or clavate	3–6(10) per oogonium, usually diclinous. Antheridial stalks entwining oogonial stalk. Antheridial cells clavate, crook-necked
Oospores	1 per oogonium, plerotic, 16.3–25 µm (av. 18.7 µm) in diameter	1 per oogonium, aplerotic, 7–22 µm (av. 14.5 µm) in diameter	1 per oogonium, plerotic, (13)16–25(30) µm (av. 20 µm) in diameter	1 per oogonium, plerotic, 10–21 µm in diameter	1–2 per oogonium, plerotic, 21–34 µm (av. 27.3 µm) in diameter	1 per oogonium, plerotic, 13.2–17.5 µm in diameter	1 per oogonium, aplerotic, average 27.5 µm in diameter
Reference	This study	van der Plaats-Niterink 1981	De Cock 1986	Paul and Bala 2008	Paul 2001	van der Plaats-Niterink 1981	van der Plaats-Niterink 1981

Table 2 A comparison of *Pythium wuhanense* with related species

Character	*P. wuhanense*	*P. emineosum*	*P. kunmingense*	*P. paroecandrum*	*P. spinosum*
Growth rate on PCA	50 mm day^{-1} at 25 °C	15 mm day^{-1} at 25 °C	Unknown	20–25 mm day^{-1} at 25 °C	30–35 mm day^{-1} at 25 °C
Sporangia	Globose, sometimes cylindrical to elongated, globose sporangia 11.3–25.5 μm (av. 18.1 μm) in diameter, elongated sporangia up to 130 μm long, intercalary	Globose, 12.6–32 μm in diameter	Globose, subglobose, ovoid or limoniform, 13–23 μm (av. 19 μm) in diameter, terminal or intercalary	Globose, subglobose or ellipsoidal, 12–33 μm in diameter, terminal or intercalary	Globose or limoniform, up to 33 μm in diameter, terminal or intercalary
Oogonia	Globose, sometimes cylindrical to elongated, smooth, globose oogonia 10–20 μm (av. 17.7 μm) in diameter, elongated oogonia up to 64 μm long, sometimes provided with 1–3 hyaline papilla or blunt, digitate ornamentation, mostly intercalary and catenulate with sporangia and antheridia	Globose, cylindrical or peanut-shaped, smooth, globose oogonia 13.6–28.3 μm in diameter, elongated oogonia average 28.8 μm long, mostly intercalary	Globose, subglobose or limoniform, ornamented, 15–26 μm (av. 21 μm) in diameter, terminal or intercalary	Globose or subglobose, smooth, (14)17–24(27) μm (av. 19 μm) in diameter, mostly intercalary, often in chains	Globose or fusiform, ornamented, (14)17–21 μm (av. 18.5 μm) in diameter, terminal or intercalary
Antheridia	1–2 per oogonium, monoclinous, sessile, hypogynous, intercalary or diclinous. Antheridial cells club-shaped, fist-shaped, sometimes lobate	1–3 per oogonium, monoclinous, sessile, hypogynous, or diclinous, occasionally intercalary. Antheridial cells hardly inflated	1–3 per oogonium, mostly monoclinous. Antheridial cells clavate, curved, vermiform or sickle-shaped	1–2(5) per oogonium, monoclinous, sometimes sessile, diclinous,. Antheridial cells club-shaped	1(3) per oogonium, monoclinous. Antheridial cells hardly inflated
Oospores	1–(2) per oogonium, aplerotic, 7.5–17.5 μm (av. 14.5 μm) in diameter	1–2 per oogonium, plerotic and aplerotic, 11.9–24.4 μm in diameter	1 per oogonium, plerotic, 10–24 μm (av. 19 μm) in diameter	1 per oogonium, aplerotic, (13)15–21(23) μm (av. 17 μm) in diameter	1 per oogonium, plerotic, (13)15–19(20) μm (av. 17.2 μm) in diameter
Reference	This study	Bala et al. 2010	Yu 1973	van der Plaats-Niterink 1981	van der Plaats-Niterink 1981

morphological characteristics of *P. wuhanense* with *Pythium* sp. P19448 and *Pythium* sp. P19510, due to the lack of morphological descriptions of the two species in the paper of Robideau et al. (2011). However, in the phylogenetic tree of ITS sequences, *P. wuhanense* was more closely related to *P. spinosum* and *P. kunmingense*, but not to *Pythium* sp. P19448 and *Pythium* sp. P19510 (Fig. 6). Furthermore, *P. wuhanense* had low DNA sequence similarities with *P. spinosum* (95.1 % ITS identity with HQ643791 and 98.3 % COI identity with HQ708832), with *P. kunmingense* (94.9 % ITS identity with HQ643672 and 95.2 % COI identity with HQ708716), and with *Pythium* sp. P19448 and *Pythium* sp. P19510 (97.4–97.6 % ITS identities with HQ261737 and HQ261738, 98.5 % COI identity with HQ261484 and HQ261485). Furthermore, in morphology, *P. wuhanense*, with smooth oogonia and aplerotic oospores, differs markedly from *P. kunmingense* and *P. spinosum* with ornamented oogonia and plerotic oospores (Table 2).

In conclusion, the distinctive morphological and molecular characteristics of *P. agreste* and *P. wuhanense*, compared with all other species described in the genus *Pythium*, confirms that these two species are new to science.

Pythium species are distributed all over the world ranging from tropical to temperate and arctic regions (van der Plaats-Niterink 1981; Ho et al. 2012). There are 301 described *Pythium* species in the world (www.indexfungorum.org, 2013). including 69 species from China (Long et al. 2013). Most *Pythium* species are saprobic, but some are important pathogens of higher plants, fungi, animals, and human beings. Several are beneficial as biological control agents, as well as a source of chemicals useful in medicine and the food industry (van der Plaats-Niterink 1981; Ho et al. 2012). The study of *Pythium* from a variety of new, diverse habitats is likely to generate new species in the future.

Acknowledgments This work was supported by the National Natural Science Foundation of China (No. 31270076, 31070434), the Guangxi Natural Science Foundation (No. 2011GXNSFA018078), the Plans for Construction of Scientific Topnotch and Innovation Team in Guangxi University, the Plans for Creative Training of Post-Graduates in Guangxi University (GXU11T31078), and the Central Public-interest Scientific Institution Basal Research Fund (2012–9). We thank Dr. Jo Taylor from Royal Botanic Garden Edinburgh for revising the manuscript and comments.

References

Ali-Shtayeh MS, Saleh ASF (1999) Isolation of *Pythium acanthicum*, *P. oligandrum*, and *P. periplocum* from soil and evaluation of their mycoparasitic activity and biocontrol efficacy against selected phytopathogenic *Pythium* species. Mycopathologia 145:143–153. doi:10.1023/A:1007065010931

Allain-boulé N, Tweddell R, Mazzola M, Bélanger R, Lévesque CA (2004) *Pythium attrantheridium* sp. nov.: taxonomy and comparison with related species. Mycol Res 108:795–805. doi:10.1017/S095375620400053X

Bala K, Robideau GP, Désaulniers N, De Cock AWAM, Lévesque CA (2010) Taxonomy, DNA barcoding and phylogeny of three new species of *Pythium* from Canada. Persoonia 25:22–31. doi:10.3767/003158510X524754

Balghouthi A, Jonathan R, Gognies S, Mliki A, Belarbi A (2013) A new species, *Pythium echinogynum*, causing severe damping-off of tomato seedlings, isolated from Tunisia, France, and India: morphology, pathology, and biological control. Ann Microbiol 63:253–258. doi:10.1007/s13213-012-0468-x

Belbahri L, McLeod A, Paul B, Calmin G, Moralejo E, Spies CFJ, Botha WJ, Clemente A, Descals E, Sánchez-Hernández E, Lefort F (2008) Intraspecific and within-isolate sequence variation in the ITS rRNA gene region of *Pythium mercuriale* sp. nov. (Pythiaceae). FEMS Microbiol Lett 284:17–27. doi:10.1111/j.1574-6968.2008.01168.x

De Cock AWAM (1986) Marine Pythiaceae from decaying seaweeds in the Netherlands. Mycotaxon 25:101–110

De Cock AWAM, Lévesque CA, Melero-vara M, Serrano Y, Guirado ML, Gómez J (2008) *Pythium solare* sp. nov., a new pathogen of green beans in Spain. Mycol Res 112:1115–1121. doi:10.1016/j.mycres.2008.03.005

Guo LD, Hyde KD, Liew ECY (2000) Identification of endophytic fungi from *Livistona chinensis* based on morphology and rDNA sequences. New Phytol 147:617–630. doi:10.1046/j.1469-8137.2000.00716.x

Ho HH, Chen XX, Zeng HC, Zheng FC (2012) The occurrence and distribution of *Pythium* species on Hainan Island of South China. Bot Stud 53:525–534

Huelsenbeck JP, Ronquist F (2001) MRBAYES: Bayesian inference of phylogeny trees. Bioinformatics 17:754–755. doi:10.1093/bioinformatics/17.8.754

Hulvey J, Telle S, Nigrelli L, Lamour K, Thines M (2010) Salisapiliaceae—a new family of Oomycetes from marsh grass litter of southeastern North America. Persoonia 25:109–116. doi:10.3767/003158510X551763

Kageyama K, Senda M, Asano T, Suga H, Ishiguro K (2007) Intra-isolate heterogeneity of the ITS region of rDNA in *Pythium helicoides*. Mycol Res 6:416–423. doi:10.1016/j.mycres.2007.01.019

Karaca G, Jonathan R, Paul B (2009) *Pythium stipitatum* sp. nov. isolated from soil and plant debris taken in France, Tunisia, Turkey, and India. FEMS Microbiol Lett 295:164–169. doi:10.1111/j.1574-6968.2009.01579.x

Katoh K, Kuma K, Toh H, Miyata T (2005) MAFFT version 5: improvement in accuracy of multiple sequence alignment. Nucleic Acids Res 33:511–518. doi:10.1093/nar/gki198

Lévesque CA, De Cock AWAM (2004) Molecular phylogeny and taxonomy of the genus *Pythium*. Mycol Res 108:1363–1383. doi:10.1017/S0953756204001431

Long YY, Wei JG, Huang CL, He YQ, Yuan GQ, Shi Y, Xiong Y (2010) A new *Pythium* species isolated from vegetable fields and analysis by rDNA ITS sequence. Mycosystema 29:795–800

Long YY, Wei JG, Sun X, He YQ, Luo JT, Guo LD (2012) Two new *Pythium* species from China based on the morphology and DNA sequence data. Mycol Prog 11:689–698. doi:10.1007/s11557-011-0778-6

Long YY, Wei JG, Yun CG, Guo LD, Huang SD, Li NH, Pan XH (2013) Three new records of *Pythium* in China. Mycosystema 31 (in press)

Martin FN (2000) Phylogenetic relationships among some *Pythium* species inferred from sequence analysis of the mitochondrially encoded cytochrome oxidase II gene. Mycologia 92:711–727. doi:10.2307/3761428

Mcleod A, Botha WJ, Meitz JC, Spies CFJ, Tewoldemedhin YT, Mostert L (2009) Morphological and phylogenetic analyses of

Pythium species in South Africa. Mycol Res 113:933–951. doi:10.1016/j.mycres.2009.04.009

Moralejo E, Clemente A, Descals E, Belbahri L, Calmin G, Lefort F, Spies CFJ, McLeod A (2008) *Pythium recalcitrans* sp. nov. revealed by multigene phylogenetic analysis. Mycologia 100:310–319. doi:10.3852/mycologia.100.2.310

Nechwatal J, Oßwald WF (2003) *Pythium montanum* sp. nov., a new species from a spruce stand in the Bavarian Alps. Mycol Prog 2:73–80. doi:10.1007/s11557-006-0046-3

Nechwatal J, Wielgoss A, Mendgen K (2005) *Pythium phragmitis* sp. nov., a new species close to *P. arrhenomanes* as a pathogen of common reed (*Phragmites australis*). Mycol Res 109:1337–1346. doi:10.1017/S0953756205003990

Nylander JAA (2008) MrModeltest 2.3 README. http://www.abc.se/~nylander/mrmodeltest2/mrmodeltest2.html. Accessed 22 May 2008

Paul B (2001) A new species of *Pythium* with filamentous sporangia having pectinolytic activities, isolated in the Burgundy region of France. FEMS Microbiol Lett 199:55–59. doi:10.1111/j.1574-6968.2001.tb10650.x

Paul B, Bala K (2008) A new species of *Pythium* with inflated sporangia and coiled antheridia, isolated from India. FEMS Microbiol Lett 282:251–257. doi:10.1111/j.1574-6968.2008.01138.x

Paul B, Galland D, Bhatnagar T, Dulieu H (1998) A new species of *Pythium* isolated from the Burgundy region in France. FEMS Microbiol Lett 158:207–213. doi:10.1111/j.1574-6968.1998.tb12822.x

Robideau GP, De Cock AWAM, Coffey MD, Voglmayr H, Brouwer H, Bala K, Chitty DW, Désaulniers N, Eggertson QA, Gachon CMM, Hu CH, Küpper FC, Rintoul TL, Sarhan E, Verstappen ECP, Zhang Y, Bonants PJM, Ristaino JB, Lévesque CA (2011) DNA barcoding of Oomycetes with cytochrome c oxidase subunit I and internal transcribed spacer. Mol Ecol Resour 11:1002–1011. doi:10.1111/j.1755-0998.2011.03041.x

Senda M, Kageyama K, Suga H, Lévesque CA (2009) Two new species of *Pythium*, *P. senticosum* and *P. takayamanum*, isolated from cool-temperate forest soil in Japan. Mycologia 101:439–448. doi:10.3852/08-104

Spies CFJ, Mazzola M, Botha WJ, Langenhoven SD, Mostert L, McLeod A (2011a) Molecular analyses of *Pythium irregulare* isolates from grapevines in South Africa suggest a single variable species. Fungal Biol 115:1210–1224. doi:10.1016/j.funbio.2011.08.006

Spies CFJ, Mazzola M, Botha WJ, van der Rijst M, Mostert L, Mcleod A (2011b) Oogonial biometry and phylogenetic analyses of the *Pythium vexans* species group from woody agricultural hosts in South Africa reveal distinct groups within this taxon. Fungal Biol 115:157–168. doi:10.1016/j.funbio.2010.11.005

Sun X, Guo LD (2010) *Micronematobotrys*, a new genus and its phylogenetic placement based on rDNA sequence analyses. Mycol Prog 9:567–574. doi:10.1007/s11557-010-0664-7

Swofford DL (2002) Phylogenetic analysis using parsimony (and other methods). Version 4, Sinauer, Sunderland http://paup.csit.fsu.edu/Cmd_ref_v2.pdf

Tojo M, West PV, Hoshino T, Kida K, Fujii H, Hakoda A, Kawaguchi Y, Mühlhauser HA, Van Den Berg AH, Küpper FC, Herrero ML, Klemsdal SS, Tronsmo AM, Kanda H (2012) *Pythium polare*, a new heterothallic oomycete causing brown discolouration of *Sanionia uncinata* in the Arctic and Antarctic. Fungal Biol 116:756–768. doi:10.1016/j.funbio.2012.04.005

Uzuhashi S, Tojo M, Kobayashi S, Kakishima M (2009) *Pythium apinafurcum*: its morphology, molecular phylogeny, and infectivity for plants. Mycoscience 50:281–290. doi:10.1007/s10267-009-0486-0

van der Plaats-Niterink AJ (1981) Monograph of the genus *Pythium*. Stud Mycol 21:1–242

White TJ, Bruns TD, Lee S, Taylor J (1990) Amplification and direct sequencing of fungal ribosomal DNA genes for phylogenetics. In: Innis MA, Sninsky DH, White TJ (eds) PCR Protocols. Academic, London, pp 315–322

Yu YN (1973) Five new species of *Pythium*. Acta Microbiol Sin 13(2):116–123